18th Brazilian Congress of Thermal Sciences and Engineering
November 16-20, 2020 (Online)

ENC-2020-0676
NUMERICAL MODELLING OF VISCOSITY RATIO INFLUENCE ON TERTIARY RECOVERY BY NEWTONIAN FLUIDS INJETION THROUGH A POROUS MEDIA

Ayrton Cavallini Zotelle
Renato do Nascimento Siqueira
Instituto Federal do Espírito Santo, Department of Mechanical Engineering, Rod. BR 101 North, km 58, São Mateus, Espírito Santo, Brazil.
ayrton.zotelle1@hotmail.com
renatons@ifes.edu.br

Fábio de Assis Ressel Pereira
Universidade Federal do Espírito Santo, Department of Industrial Technology, Vitória, Espírito Santo, Brazil.
fabio.a.pereira@ufes.br

André Leibsohn Martins
Petrobras, Horácio Macedo street 950, Ilha do Fundão Cidade Universitária, CEP 21941-915, Rio de Janeiro, Rio de Janeiro, Brazil.
aleibsohn@petrobras.com.br

Abstract. *In many cases in the oil industry, the application of primary and secondary recovery methods present low efficiency, especially on reservoirs that contain high viscosity oils. In those cases, the application of the tertiary recovery method comes to increase the recovery factor. Among the parameters that influence the recovery efficiency is the viscosity ratio. This work uses the CFD technique to evaluate the viscosity ratio influence on the tertiary recovery efficiency by the injection of Newtonian fluids through a porous media. The Ansys FLUENT® 16.0 is used to perform the simulations, the Porous Media model to represent the domain and the VOF model to describe the fluids. The simulation results match with the experimental data and permit the evaluation of the displacement behaviour inside the porous media as well.*

Keywords: *tertiary recovery, porous media, viscosity ratio.*

1. INTRODUCTION

Despite the increasing use of renewable source of energy, other ways to improve the recovery factor of oil reservoirs have been develop to match the increasing energy consumption. One of them is the tertiary, or non-conventional, recovery method.

At the beginning of the production of a petroleum reservoir, it usually has enough energy to raise the oil to the surface. This process is called primary recovery. As the oil is removed from the reservoir, an energy depletion occurs and other methods must be employed to bring the oil to the surface.

The injection of a fluid on the reservoir to displace the oil is a frequent method used to increase the volume of recovered oil, mainly in the reservoirs that contain high viscosity oils. Therefore, understanding the problem of fluid flow in porous media is of utmost importance in order to maximize the amount of oil recovered (Souza, 2018). The water and gas injection is called secondary recovery and the tertiary recovery, also called non-conventional recovery method, uses polymer, water vapor and surfactants as injection fluid.

The efficiency of fluid displacement during the oil recovery process is a direct consequence of the interfacial characteristics of the fluids. In this system, the displacer fluid penetrates the oil phase, forming fingers, which represent a preferential flow, causing much of the oil to remain trapped inside the reservoir (Lenormand et al., 1988). The viscosity ratio between the injection and displaced fluid and capillary number are some of the parameters that influence on the displacement pattern inside the porous media. Studies in the literature shows that the displacement efficiency is independent of the capillary number when this parameter becomes high (Soares et al., 2005; Soares et al. 2015; Souza, 2018). In these cases, the viscosity ratio is the only responsible of the changes of the displacement efficiency.

Besides various studies on the literature that evaluate the influence of these parameters, due the complexity to control de viscosity ratio between the fluids, a few studies evaluate the influence of the viscosity ratio on the oil

displacement and the recovery efficiency. Therefore, this work investigates, by CFD, the influence of the viscosity ratio on tertiary recovery efficiency and on the displacement pattern between the displaced fluid and the injected fluid.

The use of the CFD technique promotes a way to investigate the fluid behaviour during the recovery process and evaluate the changes of the recovery factor promoted by the changes of the flow pattern inside the porous media. These analyses can assist the fluid selection to ensure a better recovery efficiency on the process.

2. METHODOLOGY

2.1 Governing equations

To represent the effects of porosity and permeability on the flow, the Porous Media model is used. In this model, the concept of physical velocity (Equation 1) is used to represent the increase in velocity, due to the reduction of the useful area of the flow, expressed by:

$$v_f = \frac{v_s}{\phi}, \tag{1}$$

where v_f is the physical velocity, ϕ is the porosity of the porous medium and v_s is the superficial velocity (relation of the volumetric flow and the face area of the cell mesh). A source term (S_ϕ) of Darcy's equation is introduced in the momentum equation to interpret the effects of the porous medium permeability, expressed by:

$$S_\phi = -\left(\frac{\mu}{k} \vec{v}_f + C_2 \frac{1}{2} \rho |v_f| \vec{v}_f \right), \tag{2}$$

where μ is the dynamic viscosity, k is the absolute permeability, ρ is the fluid density and C_2 is Forchheimer term.

The VOF model is used to represent the interface between the fluids. In this model, the phases are treated as continuous and immiscible and a unique set of continuity and momentum equation is solved to the both phases and the volume fraction of each phase is tracked along the domain.

The continuity equation and momentum equation for a flow through a porous media, modeled by the VOF multiphase model are show in equations 3 and 4.

$$\frac{\partial(\phi\rho)}{\partial t} + \nabla \cdot \left(\phi \rho \vec{v}_f \right) = 0, \tag{3}$$

$$\frac{\partial(\phi\rho \vec{v}_f)}{\partial t} + \nabla \cdot \left(\phi \rho \, \vec{v}_f \vec{v}_f \right) = -\nabla P + \nabla(\phi \vec{\tau}) + \phi \rho \, g + \phi \vec{F}_\sigma + \vec{S}_\phi, \tag{4}$$

where $\vec{\tau}$ is the stress tensor and $\vec{F}_\sigma$ is the term that represents the surface tension forces on the fluid interfaces, calculated by:

$$F_\sigma = \sigma \frac{\rho \kappa \nabla \alpha_1}{\frac{1}{2}(\rho_1 + \rho_2)}, \tag{5}$$

σ is the interfacial tension, the subscribed 1 and 2 represents the primary and secondary phase, respectively, and κ is the fluid interface curvature, calculated by Equation 6:

$$\kappa = -(\nabla \cdot \hat{n}), \tag{6}$$

where $\hat{n}$ is the unit vector normal to the fluids interface. In the cells of the mesh adjacent to the wall, the interface vector is calculated by:

$$\hat{n} = \hat{n}_w \cos(\theta_w) + \hat{t}_w \sin(\theta_w), \tag{7}$$

$\hat{n}_w$ and $\hat{t}_w$ are the unit vector normal and tangential to the wall, and θ_w is the wall adhesion angle. The volume fraction (α) of each phase is given by:

$$\frac{\partial \alpha}{\partial t} + \vec{v}_f \cdot \nabla \alpha = 0 \cdot \tag{8}$$

The fluid properties on all cells are representative of a unique fluid or a mixture of fluids, depending of the volume fraction of the fluids on the cell (ANSYS, 2013). On the cells that contain only one fluid, the properties used to solve the governing equations are the fluid properties, and those cells that contain a parcel of each fluid, the properties are obtained by the volume fraction weighted average of the fluids property on the cell. In the multiphase flow, $N - 1$ volume fraction equations are solved, where N is the number of phases on the flow.

Some parameters are used to measure the displacement efficiency. One of them is the lost mass (m_e) that represent the fraction of the oil mass that remain inside the porous media on the breakthrough time (m_p), and the oil mass inside the porous media when the recovery process started (m_t). The breakthrough, represent the moment when the first volume of injected fluid crosses the outlet boundary, therefore producing not only oil anymore, but also some injected fluid. The lost mass is determinate by:

$$m_e = \frac{m_p}{m_t}, \tag{9}$$

and the viscosity ratio between the injected and displaced fluid (N_μ) and the capillary number (Ca) are define as:

$$N_\mu = \frac{\mu_d}{\mu_i}, \tag{10}$$

$$Ca = \frac{\mu_d U}{\sigma}, \tag{11}$$

where μ_d and μ_i are the displaced and injected fluid viscosity, respectively, U is the injection velocity and σ is the interface tension between the fluids.

2.2 Geometry and mesh

The numerical model used in this study is based on the experimental approach of Souza (2018), see Fig. 1. The porous media have a cylindrical shape, with 35 mm diameter, 70 mm long and the outlet section is a tube with 12 mm diameter. The tridimensional CAD model used on the numerical simulations is shown on Fig 1.

1. Storage tank;
2. Fixed part of the hydraulic press;
3. Hydraulic activator;
4. Hydraulic piston;
5. Moved part of the hydraulic press;
6. Inlet valve of the hydraulic activator;
7. Outlet valve of the hydraulic activator;
8. High pressure tube;
9. Metallic pipe;
10. Porous media;
11. Relief valve;
12. Low pressure tube;
13. Outlet valve of the porous media;

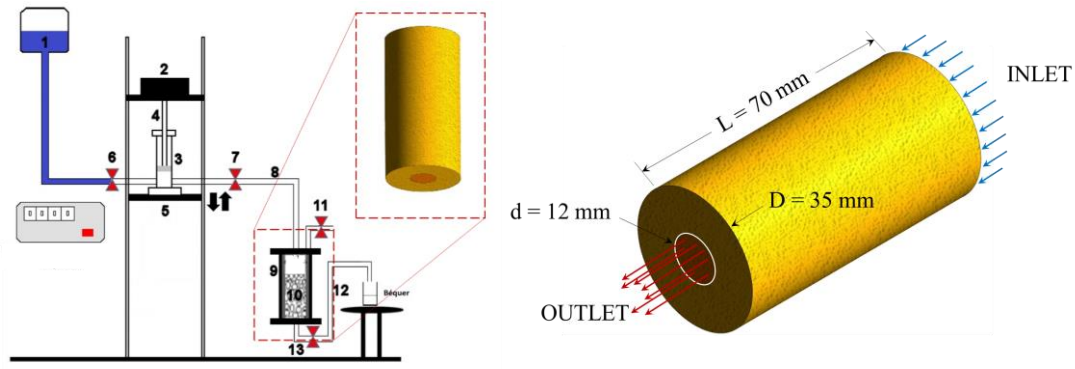

Figure 1. Geometry used on the simulations perform.

The mesh shows hybrid characteristics, structured on the axial direction, with 140 divisions, and non-structured on the cross section, with a maximum element size of 0.25 mm and 1.8 million hexagonal and tetragonal elements. More details about the mesh are shown on Figure 2.

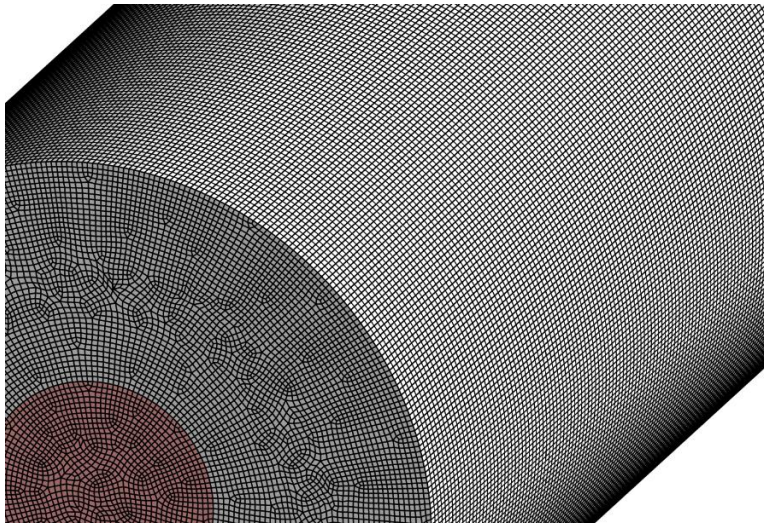

Figure 2. Computational mesh.

The MultiZone method was used to limit the mesh format to hexa/tetra elements. The final mesh has a maximum element quality of 0.925, minimum element quality of 0.330 and a maximum aspect ratio of 17.3.

2.3 Boundary conditions and porous medium and fluid properties

The domain was treated as a homogenous porous media, with porosity $\phi = 0.372$ and absolute permeability $k = 28.64 Da$, based on Souza (2018). The Reynolds number was kept low, therefore, the Forchheimer term (quadratic term of Equation 2) is equal to 0, and the capillary number is high enough to the capillary effects on the displacement process are negligible.

The initial condition considered that the porous media is fully saturated with oil (displaced fluid). The displacer fluid was injected with a constant volumetric flow $q = 3.28\, mL/\min$ on the inlet, and the outlet pressure was considered equal to 0 Pa and the other boundaries were considered as walls. Several fluids were selected to perform the numerical simulations based on Souza (2018) analyses. The properties of the displaced and the injected fluids, as well the viscosity ratio and surface tension between the fluids are presented in Tab. 1.

Table 1. Fluid characteristics for the different viscosity ratio evaluated.

N_μ	**Injected fluid**		**Displaced fluid**		$\sigma\,(mN/m)$	Ca ($x10^{-3}$)
	$\rho\,(kg/m^3)$	$\mu\,(mPa\ s)$	$\rho\,(kg/m^3)$	$\mu\,(mPa\ s)$		
40.10	907.1	2.53	929.2	103.1	3.89	4.05
21.82	907.1	2.53	916.8	55.0	5.50	1.53
8.20	933.1	9.80	922.9	81.0	3.86	3.20
4.40	931.2	12.50	916.8	55.0	6.43	1.31
2.20	939.0	24.90	916.8	55.0	5.60	1.50
0.93	990.6	81.30	922.9	81.0	4.60	2.69
0.50	1036.6	111.0	916.8	55.0	4.72	1.78

Due to the lack of information on the contact angle with the different combinations of fluids used on the experimental approach of Souza (2018), the contact angle (θ_w) used to perform the simulations was 90º. Therefore, both phase do not wet the wall boundaries.

2.4 Solver parameters

The numerical treatment of a displacement process through a porous media is complex. Therefore, the correct selection of the spatial and transient discretization schemes is extremely important. The studies of Santos et al. (2016) was used to help on the algorithms selection. The multiphase model parameters and solution methods are show on Tab. 2.

Table 2. Solver parameters for performing the numerical simulations.

Multiphase model	Model		VOF
	Volume fraction formulation		Explicit
	Surface tension		Constant
Solution Method	Time step		0.20 s
	Pressure-velocity coupling		PISO
	Spatial discretization	Gradient	Least Squares Cell Based
		Moment	QUICK
		Volume fraction	CICSAM
	Transient formulation		First order

3. RESULTS AND DISCUSSIONS

To a better comparison of the numerical data with the experiments, a regression analysis of the experimental results of Souza (2018) were made in order to determinate a prediction band, with 95% of reliability. The comparison of the lost mass obtained on the experimental approach of Souza (2018) and the results obtained by the numerical simulation at the breakthrough time are shown on Fig. 3.

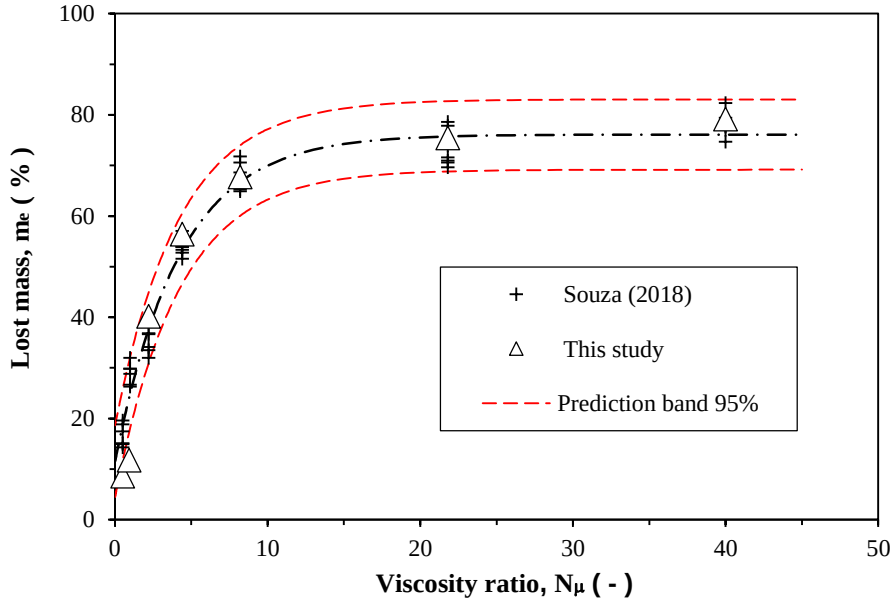

Figure 3. Effect of viscosity ratio on lost mass at breakthrough time.

On Fig. 3, it is possible to note that the lost mass tends to an asymptotic behaviour when the viscosity ratio increases and the results of the numerical modelling fit well the experimental data, except those that the viscosity ratio becomes lower than one. Most results of lost mass were among the 95% prediction band, but for low values of viscosity ratio, the numerical model presents lower values of lost mass when compared with the experimental data. This occurs because the numerical model is unable to represent the parcel of oil that remains adhered to the grains of the porous medium.

Small values of viscosity ratio have greater displacement efficiencies and when the viscosity ratio is larger than 20, the lost mass is almost constant. This behaviour was already reported by Soares et al. (2005), Souza (2018) and Gu et al. (2018).

The decrease of the lost mass as the viscosity ratio decrease occurs due the increase of the shear stress developed by the injected fluid on the displaced fluid. The volume of oil remaining on the porous media decrease with the increase of the shear stress and when the shear stress is low, the injected fluid has low displacement efficiency and higher values of lost mass are noticed.

The divergences between the lost mass numerical and experimental results at low viscosity ratios, as shown on Fig 3, occurs due to the fact that the numerical model considered the porous media perfectly homogenous, where the solid and fluid phases are not differed. On a real case, the pores can be not interlinked, resulting on the entrapment of oil parcels on the porous media, where the injected fluid is unable to displace the oil. The heterogeneous characteristics of the porous media make the volume of oil trapped on the porous media to increase, due the fact that injected fluid does not reach this parcels of oil.

The viscosity ratio affects the lost mass, as well the displacement pattern of the fluids inside the porous media. The CFD permit to visualize the fingering formation on the porous media, which is difficult to visualize on the experimental approach. The fingering formation is shown on Fig. 4.

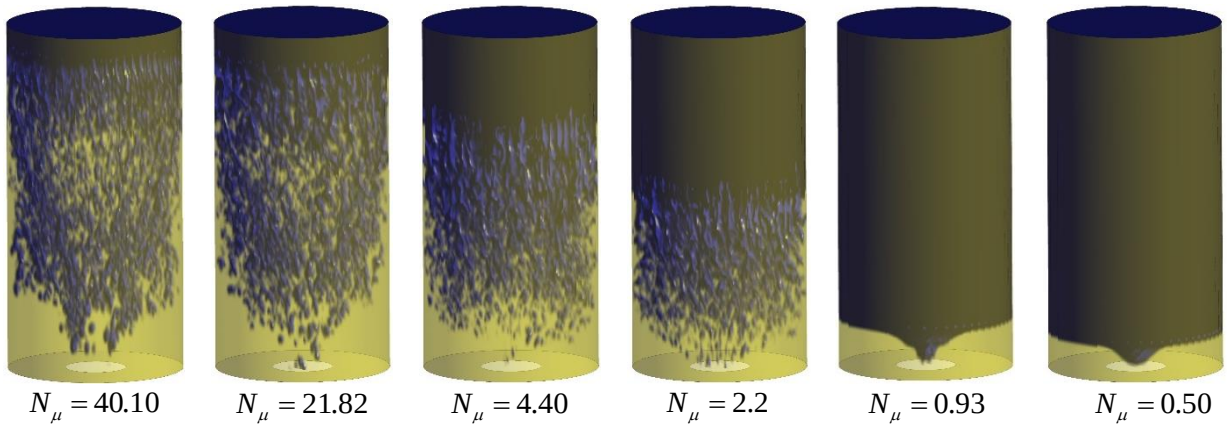

Figure 4. Fingering formation inside the porous media at different viscosity ratio.

At large viscosity ratios, the displacer fluid is disperse inside the porous media, as show Fig. 4. This characteristic is because at high viscosity ratios, the displacement pattern is the viscous finger, characterized by the appearance of preferential paths. When the viscosity ratio decrease, it is possible to note that de displacement transit between the viscous finger and stable displacement patterns.

When the dynamic viscosity of the injected fluid approaches the dynamic viscosity of the displaced fluid, the viscous force acting on the injected fluid is larger, contributing to the increase in the amount of liquid flowing out of the porous medium, leading to a decrease in the lost mass fraction. These results are in accordance with those obtained by Soares et al. (2015) and Souza (2018).

The capillary finger pattern was not evidenced on the simulations. This occurs because the capillary number is larger than the values are noted. This behaviour is also in accordance with the literature (Lenormand et al., 1988; Zhang et al., 2011; Souza, 2018).

4. CONCLUSION

The results show that the numerical model was able to appropriately describe the physical phenomenon of oil displacement through a porous media and the asymptotic behaviour of the lost mass as a function of the viscosity ratio. It was able to note that low values of viscosity ratio have a better displacement efficiency, reducing the residual volume of oil that remain inside the porous media. Besides the determination of the lost mass, the simulations also allowed to evaluate the displacement behaviour of the fluid inside the porous media, contributing with the understanding of the phenomenon and the increase in the recovery factor.

5. ACKNOWLEDGEMENTS

The authors would like to thank PETROBRAS for the financial support to carry this research and the Instituto Federal do Espírito Santo (IFES) and Universidade Federal do Espírito Santo (UFES) for the structure to develop this research.

6. REFERENCES

Ansys, Inc. 2013. *Ansys fluent theory guide*. Release 15.0. Canonsburg, PA: ANSYS, Inc.

Gu, Q.; Liu, H.; Zhang, Y. Lattice Boltzmann Simulation of Immiscible Two-Phase Displacement in Two-Dimensional Berea Sandstone. *Applied Sciences*, [S.l.], v. 8, n. 9, p. 1497-1510, 31 ago. 2018.

Lenormand, R.; Touboul, E.; Zarcone, C. Numerical models and experiments on immiscible displacements in porous media. *Journal of fluid mechanics*, Cambridge University Press, v. 189, p. 165-187, 1988.

Santos, K. B.; Romero, O. J.; Meneguelo, A. P.; Ribeiro, D. C. A numerical investigation of immiscible water-oil displacement in simplified porous media. *IEEE Latin America Transactions*, [S.l.], v. 14, n. 5, p. 2175-2183, maio 2016. Institute of Electrical and Electronics Engineers (IEEE).

Soares, E. J.; Carvalho, M. S.; Mendes, P. R. S. Immiscible Liquid-Liquid Displacement in Capillary Tubes. *Journal of Fluids Engineering*, [S.l.], v. 127, n. 1, p. 24-31, 1 jan. 2005. ASME International.

Soares, E. J.; Thompson, R. L.; Niero, D. C. Immiscible liquid–liquid pressure-driven flow in capillary tubes: experimental results and numerical comparison. : Experimental results and numerical comparison. *Physics of Fluids*, [S.l.], v. 27, n. 8, p. 1-14, ago. 2015. AIP Publishing.

Souza, A. W. Q. *Avaliação da eficiência de recuperação de um líquido contido em um meio poroso por injeção de líquidos newtonianos e não-newtonianos.* 2018. 79 p. Dissertação (Mestrado) - Curso de Engenharia Mecânica, Departamento de Pós-graduação em Engenharia Mecânica, Universidade Federal do Espírito Santo, Vitória, 2018.

Zhang, C; Oostrom, M.; Wietsma, T. W.; Grate, J. W.; Warner, M. G. Influence of Viscous and Capillary Forces on Immiscible Fluid Displacement: pore-scale experimental study in a water-wet micromodel demonstrating viscous and capillary fingering. : Pore-Scale Experimental Study in a Water-Wet Micromodel Demonstrating Viscous and Capillary Fingering. *Energy & Fuels*, [S.l.], v. 25, n. 8, p. 3493-3505, 18 ago. 2011. American Chemical Society (ACS).

7. RESPONSIBILITY NOTICE

The authors are the only responsible for the printed material included in this paper.